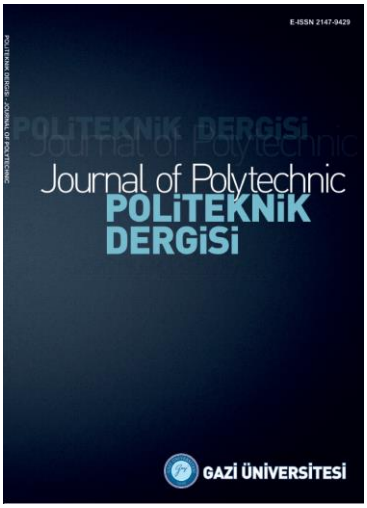

POLİTEKNİK DERGİSİ

JOURNAL of POLYTECHNIC

ISSN: 1302-0900 (PRINT), ISSN: 2147-9429 (ONLINE)
URL: http://dergipark.org.tr/politeknik

Practical radial distribution feeder for techno economic in ders based on ann and chameleon optimization algorithms

Ysa ve bukalemun optimizasyon algoritmalarına dayalı der'lerde tekno ekonomik için pratik radyal dağıtım besleyicisi

Yazar(lar) (Author(s)): *Jemaa BOJOD[1], Bilgehan ERKAL[2]*

ORCID[1]: 0009-0002-4003-8145

ORCID[2]: 0000-0002-1405-6932

To cite to this article: Bojod J., Erkal B., "Practical radial distribution feeder for techno economic in ders based on ann and chameleon optimization algorithms", ***Journal of Polytechnic***, 26(3): 1285-1297, (2023).

Bu makaleye şu şekilde atıfta bulunabilirsiniz: Bojod J., Erkal B., "practical radial distribution feeder for techno economic in ders based on ann and chameleon optimization algorithms", ***Politeknik Dergisi***, 26(3): 1285-1297, (2023).

Erişim linki (To link to this article): http://dergipark.org.tr/politeknik/archive

DOI: **10.2339/politeknik.1348672**

Practical Radial Distribution Feeder for Techno Economic in DERs based on ANN and Chameleon Optimization Algorithms

Highlights

- *This study uses artificial neural networks and the Chameleon Optimization Algorithm to analyze the best integration of renewable energy sources and electric vehicles in distribution feeders.*
- *The proposed method reduced the power loss, regulate voltage levels, and decrease the cost and emissions under unpredictable load demand.*
- *In this study, the generated output power of the models is compared to solar photovoltaic generation systems and wind turbine generation systems.*

Graphical Abstract

ANN and COA are used in this study to determine the optimal parameters of the objective function and EV installation tasks simultaneously to lower power loss and overall costs. The summary of this study is shown in following figure.

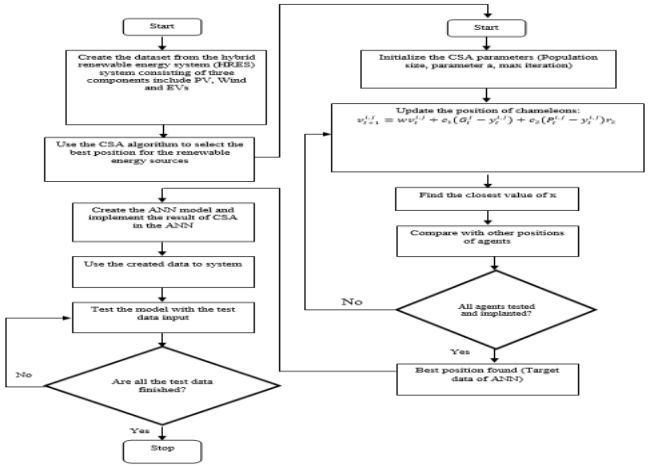

Figure. Flowchart of the proposed method

Aim

The main aim of this study is uses artificial neural networks and the Chameleon Optimization Algorithm to analyze the best integration of renewable energy sources and electric vehicles in distribution feeders to reduce power loss, regulate voltage levels, and decrease the cost and emissions under unpredictable load demand.

Design & Methodology

The 28-bus rural distribution network in feeders is used to test the suggested methodology.

Originality

A fitness function with several objectives has been developed to reduce total active power loss while also reducing total cost and emissions generation. The study took into account the influence of EV charging/discharging behavior on the distribution system.

Findings

Final analysis of the numerical results showed that the Artificial Neural Network and Chameleon Optimization Algorithms outperformed in terms of power loss (440.94 kw) and average purchase of real power (2224 kw), but these parameters do not favor the other optimization algorithms.

Conclusion

This study evaluates whether DER integration into the distribution system is technologically, economically, and ecologically feasible. In order to solve this issue with distribution system planning, the ideal placements and sizes of PVGS, WTGS, and EVs were determined for 28 bus networks using the ANN and COA.

Declaration of Ethical Standards

The authors of this article declare that the materials and methods used in this study do not require ethical committee permission and/or legal-special permission.

YSA ve Bukalemun Optimizasyon Algoritmalarına Dayalı DER'lerde Tekno Ekonomik için Pratik Radyal Dağıtım Besleyicisi

Araştırma Makalesi / Research Article

Jemaa BOJOD*, Bilgehan ERKAL

Department of Electrical and Electronics Engineering, Karabuk University, Karabuk

(Geliş/Received : 23.08.2023 ; Kabul/Accepted : 15.09.2023 ; Erken Görünüm/Early View : 21.09.2023)

ÖZ

Dağıtılmış enerji kaynakları (DER'ler), yük merkezlerine yakın yük talebini karşılamak için daha iyi bir seçimdir. Optimum DER yerleşimi ve DER değerleri, güç kaybının azaltılmasına, voltaj profilinin iyileştirilmesine, çevre dostu olmasına, güvenilirliğe ve sistem değişikliklerinin ertelenmesine yol açar. Bu çalışma, güç kaybını azaltmak, voltaj seviyelerini düzenlemek ve öngörülemeyen yük talebi altında maliyet ve emisyonları azaltmak amacıyla yenilenebilir enerji kaynaklarının ve elektrikli araçların dağıtım besleyicilerindeki en iyi entegrasyonunu analiz etmek için yapay sinir ağlarını ve Bukalemun Optimizasyon Algoritmasını kullanmaktadır. Bu çalışmada modellerin üretilen çıkış güçleri güneş fotovoltaik üretim sistemleri ve rüzgar türbini üretim sistemleri ile karşılaştırılmıştır. Sonuç olarak, toplam aktif güç kaybını azaltırken aynı zamanda toplam maliyeti ve emisyon üretimini de azaltmak için çeşitli hedefleri olan bir uygunluk fonksiyonu geliştirilmiştir. Çalışma, EV şarj/deşarj davranışının dağıtım sistemi üzerindeki etkisini dikkate aldı. Önerilen metodolojiyi test etmek için fiderlerdeki 28 otobüslü kırsal dağıtım ağı kullanılmıştır. Sayısal sonuçların son analizi, Yapay Sinir Ağı ve Bukalemun Optimizasyon Algoritmalarının güç kaybı (440,94 kw) ve ortalama gerçek güç alımı (2224 kw) açısından daha iyi performans gösterdiğini ancak bu parametrelerin diğer optimizasyon algoritmalarını desteklemediğini gösterdi. Bu, önerilen stratejinin hem uygulanabilir hem de etkili olduğunu gösterdi.

Anahtar Kelimeler: Pratik radyal dağıtım besleyici, tekno-ekonomik, dağıtılmış enerji kaynakları, yapay sinir ağı, bukalemun optimizasyon algoritması.

Practical Radial Distribution Feeder for Techno Economic in DERs based on ANN and Chameleon Optimization Algorithms

ABSTRACT

Distributed energy resources (DERs) are a better choice to meet load demand close to load centers. Optimal DER placement and DER ratings lead to power loss reduction, voltage profile improvement, environmental friendliness, dependability, and postponement of system changes. This study uses artificial neural networks and the Chameleon Optimization Algorithm to analyze the best integration of renewable energy sources and electric vehicles in distribution feeders to reduce power loss, regulate voltage levels, and decrease the cost and emissions under unpredictable load demand. In this study, the generated output power of the models is compared to solar photovoltaic generation systems and wind turbine generation systems. As a result, a fitness function with several objectives has been developed to reduce total active power loss while also reducing total cost and emissions generation. The study took into account the influence of EV charging/discharging behavior on the distribution system. The 28-bus rural distribution network in feeders is used to test the suggested methodology. Final analysis of the numerical results showed that the Artificial Neural Network and Chameleon Optimization Algorithms outperformed in terms of power loss (440.94 kw) and average purchase of real power (2224 kw), but these parameters do not favor the other optimization algorithms. This showed that the proposed strategy is both viable and effective.

Keywords: Practical radial distribution feeder, techno-economic, distributed energy resources, artificial neural network, chameleon optimization algorithm.

1. INTRODUCTION

The integration of photovoltaic systems into distribution networks is rapidly expanding as a result of the continually rising electrical energy demand, even though it has a substantial impact on the power quality of the network [1][2]. In order to increase system efficiency, lower noise pollution, minimize carbon emissions, and lessen reliance on foreign energy sources, more and more nations are turning to RESs, which are popular examples of microturbine, biomass, wind, and solar power [3]. Recent years have seen an increase in demand for RESs due to their benefits [4][5][6]. One of the frequently recommended sources of electricity is Electric vehicles (EVs) that can lower oil consumption and emissions, even during system peak times. Gridable automobiles are

*Sorumlu yazar(Corresponding Author)
e-posta : jeamh.1985@gmail.com

expected to have a successful future due to their greater power and environmental characteristics [7][8].

The literature has conducted various studies on the mentioned title that can be divided into two types: general and specialized. The integration problem is resolved in the first instance using a single objective function, while the integration problem for DER is resolved in the second instance using a multi-objective framework [7][8].

By considering power losses, Rau and Wan proposed the idea of optimal power distribution in sub- and distribution-level transmission networks. According to the literature [9][10], there are different strategies to deal with DER integration issues with a single aim. Among the methodologies used are genetic algorithms (GA), improved learning-based optimization (ILBO), and vaccine-enhanced AI systems (Vaccine-AIS), as well as evolutionary programming (EP), mixed integer nonlinear programming (MINLP), analytical-based approaches, and artificial intelligence techniques like MINLP, ILBO, and Vaccine-AIS [11][12]. Literature data points to the presence of numerous studies that make various attempts to tackle the multi-objective problem of DER integration. Analytically based methods are used in AI techniques including PSO, MOABC, MOPSO, GA, and non-dominated swarm optimization (NSO) [13][14].

A few recent publications on DER integration-based distribution systems are also mentioned here. When an on-load tap changer (OLTC) transformer is present, shunt capacitances and dispatchable DGs can be built to minimize annual energy losses and voltage fluctuations [15][16]. The moth search optimization (MSO) algorithm was updated by Singh *et al*. to solve the issue of determining the best placement of the two simultaneously [17][18].

Elephant herding optimization and multicriteria decision-making were used to solve the optimal DERs in corporate problems in a multi-objective framework by [19]. DERs and shunt capacitors may be placed in the most efficient locations and sizes for both economic and environmental reasons using an updated PSO algorithm [20][21]. Using a multi-objective index and an analytical approach, the DER integration issue was resolved by taking into account a demand-response program to lessen both active and reactive power losses. According to [22][23], a best placements and sizes of renewable-based DGs were assessed using a newly developed voltage stability and quick PSO algorithm. Network reconfiguration and RESs integration problems were solved concurrently by Hesaroor and Das [24]. Tie-switch positions, as well as DG locations and sizes, have been optimized simultaneously to reduce yearly energy loss and benefit from cost savings [25][26].

In researches [27][28] demonstrates that many authors have discussed the topic of installing DER distribution networks to reduce power loss and benefit financially. To choose where and how big to make their DERs, they employed a number of techniques. Scientists are quite concerned about this issue because it has received so little attention. Due to the availability of renewable energy sources and electric vehicles, it has been determined that the majority of scholars overlooked the fact that each bus has a 24-hour need. The combination of power loss, overall cost, and emissions creation is a research gap in the literature needs further investigations [29][30][31]. This is why a multi-objective fitness function addressed by Artificial Neural Network (ANN) and Chameleon Optimization Algorithm (COA) with the existence of RESs and charging/discharging of EVs with unknown load requirements over 24 hours that has been adopted. This optimization strategy has been effectively applied in past applications for economic load dispatch, unit commitment, and transmission network expansion planning. This enables the authors to address a distribution system planning challenge of this scale by putting their theories into practice. The honeybee's innate propensity to search for food served as inspiration for the usage of this meta-heuristic technique. With a compounded convergent rate and quick convergence, it can solve nonlinear limited problems. It also has a reduced number of configurable controllers. This strategy is regarded as the preferable method of resolving this issue because of these advantages. Its most important contributions include the following:

1. Installation of diverse RESs with changing power factors and time-varying load demands under probabilistic power generation is made easier with a new multi-objective fitness function.
2. Aside from that, this research considers the influence of EV charging and discharging on the distribution network, as well as varying customer load demand.

Among other things, the author addresses the following topics:

1. Use of the ANN and COA to discover the best possible locations and appraisals for RESs and EVs in the distribution feeder.
2. Calculating the likelihood of wind speed and solar irradiation by using a mathematical model for each. As a result, it is possible to calculate the anticipated output power. the concept of recharging and discharging EVs is taken into account.
3. Analysis of different costs, including active power purchase cost, WTGS, PVGS installation, and O&M costs.
4. Following grid integration of RESs and electric vehicles, total network cost.

The methodology provided in this paper is applied to the following networks: A 28-bus practicable distribution network and a techno-socioeconomic study have been conducted to represent the practicality of the suggested approach. For better exemplification, the following highlights the innovation of the paper:

- To determine the current, voltage, and power loss of the distribution network, a backward/forward load flow method was created.
- An unknown daily load requirement for each bus is taken into account to make the problem seem more real.

- The development of mathematical models for the production of solar and wind energy, as well as the notion of EV charging and discharging.

The COA is used in this paper to determine the best allocations and number of DERs to connect to the distribution system while accounting for the unpredictability of load.

This is a novel meta-heuristic optimization strategy and was inspired by chameleons' foraging behavior. The method has several goals, including overall active power loss, total cost, and minimizing grid emissions under unpredictable loads.

The COA has a few controllable parameters. It is impressive at resolving composite non-linear constraint issues as demonstrated by its rapid rate of convergence. These benefits have led to its selection as a favored approach to solving these issues.

The rest of this manuscript is arranged as follows: In section 2, the mathematical problem formulation is provided as a multiobjective function with operational constraints. Section 3 of this research shows RESs and the charging/discharging feature of EVs during 24 hours. It is explained in detail in Section 4 in terms of how to use the COA and ANN to achieve the optimal parameters used in the fitness function to be decreased, as well as the fitness value and the cos function in power systems. Section 5 discusses the simulation's results while Section 6 concludes the study. Finally, the conclusion summary is closing the article followed by list of recent references.

2. MATERIAL and METHOD

This section explains the formulation of the objective function for the optimization of exploited components (PV, wind, and EV) along with the concept of ANN and the COA.

2.1. Proposed Mathematical Problem Formulation

An effort has been made to incorporate a variety of power sources into the feeders for distribution due to the erratic nature of demand. To determine the ideal locations and sizes of different power sources (cost, loss of electricity, and pollutant generation are the main goals), a fitness function that combines many objectives into one fitness function has been developed. The weighting factor rule is used to simultaneously decrease the number of critical objectives. Using Equation. (1), the stochastic multi-objective optimization problem can be modeled [22]:

$$Minimization\ F = w1 \times \underbrace{\left(\begin{matrix} C_p + PV\_instt + PV\_OM + W\_instt + W\_OM \\ + \sum_{t=1}^{24} C_{EV}(t) \end{matrix}\right)}_{Total\ Cost} + w2 \times \sum_{t=1}^{24} P_{TLoss}(t) + w3 \times \sum_{t=1}^{24} E_{emission}(t) \quad (1)$$

While, the actual cost of purchasing power (Cp) from the grid is used to calculate the fitness function's first term using Equation (2) [22].

$$C_p = \sum_{y=1}^{yr} PW^y \times 365 \times \sum_{t=1}^{24} \rho_E(t) \times P_{real}(t) \quad (2)$$

Present worth (PW) can be determined as PW = (1 + infR) / (1 + intR), where yr denotes the number of years (20 years).

The PVGS installation cost (PV_instt) is represented by the fitness function's second term, which is evaluated by Equation. (3).

$$PV\_instt = PV_{purchase\ cost} + PV_{installation\ fee} = PV_{out} \times CP_{PV} + 0.5 * (PV_{out} \times CP_{PV}) \quad (3)$$

Equation (4) is used to calculate the operation and maintenance costs for the PVGS.

$$PV\_O\&M = \sum_{y=1}^{yr} PW^y \times 0.02 \times PV\_instt \quad (4)$$

The fourth part of the main fitness function, the WTGS installation cost (W_instt), is calculated using (5).

$$W\_instt = WTpurchase\ cost + WTinstallation\ fee$$
$$W\_instt = P_w \times CP_w + 0.25 * (P_w \times CP_w) \quad (5)$$

Calculating $W\_O\&M$, also known as WTGS operation and maintenance costs (WTGS O&M), can be done using Equation (6).

$$W\_O\&M = \sum_{y=1}^{yr} PW^y \times 0.05 \times W\_instt \quad (6)$$

The sixth part of the main fitness function shows the cost of charging and discharging an electric vehicle. Car owners must choose how to charge and discharge their vehicles in order to get the most out of them. It follows its typical to declare energy one day in advance when living in an area with a deregulated electricity market. As a result, it might be called:

$$C_{EV}(t) = \rho_E(t)[\eta_{dch} P_{dch}(t) - \eta_{ch} P_{ch}(t)] \quad (7)$$

The seventh term is a representation of the total active power losses (P_TLoss) over a 24-hour period for each distribution system segment. Consider Equation (8) instead, to put it another way as mathematically expressed.

$$P_{TLoss} = \sum_{\substack{i=1 \\ i \neq j}}^{j} P_{Loss}(i,j) \quad (8)$$

The distribution segment i-j with series resistance is termed Rij, whereas the distribution segment i-j with reactance is Xij. Figure 1 depicts a power radial distribution feeder branch that is functionally comparable.

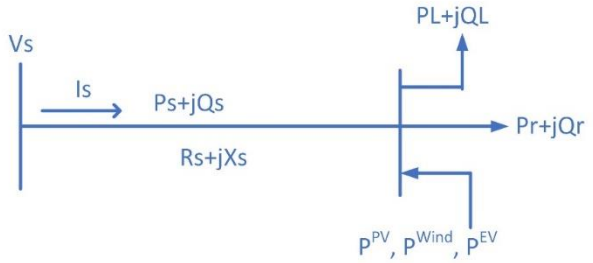

Figure 1. Diagram of an equivalent radial distribution feeder branch

Emissions during 24 hours are calculated using the following formula (9).

$$E_{EMSN} = \sum_{t=1}^{24} P_{real}(t) \times (\widehat{CO_2} + \widehat{NO_X} + \widehat{SO_2}) \quad (9)$$

The active and reactive power flow is evaluated from branch I to branch j using Equations (10) and (11).

$$P_{ij} = P_j^F + P_{jL} - P_j^{WT} - P_j^{PV} - P_j^{V2G} + P_j^{G2V} + \frac{R_{ij}}{V_i^2}\left(P_{ij}^2 + Q_{ij}^2\right) \quad (10)$$

$$Q_{ij} = Q_j^F + Q_{jL} + \frac{X_{ij}}{V_i^2}\left(P_{ij}^2 + Q_{ij}^2\right) \quad (11)$$

As an added bonus, the voltage on the jth bus may be calculated using Equations (12). These equations are generated based on Kirchhoff's law.

$$V_j^2 = V_i^2 - 2\left(P_{ij}R_{ij} + Q_{ij}X_{ij}\right) + \frac{R_{ij}^2 + X_{ij}^2}{V_i^2}\left(P_{ij}^2 + Q_{ij}^2\right) \quad (12)$$

The active and reactive power flow across the i-j section is represented by Pij and Qij. Beyond the jth bus, active and reactive power is represented by PF and QF. PWT, PPV, PV2, and PG2V, correspondingly, reflect the actual power. The current flow between the ith and jth bus can be calculated using Equation (13).

$$I_{ij} = \sqrt{\frac{P_{ij}^2 + Q_{ij}^2}{V_i^2}} \quad (13)$$

Serially, Equations (14) and (15) are used to analyze the i-j segment's active and reactive power losses.

$$P_{\text{Loss}}(i,j) = I_{ij}^2 R_{ij} \quad (14)$$

$$Q_{Loss}(i,j) = I_{ij}^2 X_{ij} \quad (15)$$

The total power loss (P_{TLoss}) of the system may be calculated by summing up the power losses of each distribution segment of the feeder using Equation (16).

$$P_{\text{TLoss}} = \sum_{\substack{i=0 \\ i\neq j}}^{n-1} P_{\text{Loss}}(i,j) \quad (16)$$

In order to meet the demand specified in Equation (17), sufficient electricity from thermal generators, solar systems, wind farms, and electric vehicles must be developed.

$$\sum_{t=1}^{24} P_{real}(t) + \sum_{t=1}^{24} P_{WTGS}(t) + \sum_{t=1}^{24} P_{PVGS}(t) + \sum_{t=1}^{24} P_{dch}(t) - \sum_{t=1}^{24} P_{ch}(t) - \sum_{t=1}^{24} P_{Load}(t) - \sum_{t=1}^{24} P_{TLoss}(t) = 0 \quad (17)$$

Each bus' voltage must be contained within a set tolerance range considering Equation (18).

$$V_i^{min} \le V_i \le V_i^{max} i \in NB \quad (18)$$

To maintain network dependability, the rated thermal loading of each distribution segment needs to be lower than that value that can be mathematically expressed in Equation (19).

$$I_{ij} \le I_{\text{Th}}^{\text{rated}} \quad (19)$$

In order to maintain system stability, a predefined number of grid-capable vehicles come each hour for charging and discharging by using Equation (20).

$$\sum_{t=1}^{24} \text{EV}(t) \le N_{\text{EV}} \quad (20)$$

The battery capacity of grid-connected vehicles is anticipated to be able to store up to 90% of that capacity and release up to 20% of it.

It will be assumed for the purposes of this study that charging and discharging automobiles are not done simultaneously. Many assumptions were made when trying to integrate RESs with EVs as follows:

1. The system under consideration is evaluated as harmonics-free and balanced.
2. The voltage magnitude on bus number one is taken as one p.u. and regarded as a slack bus.
3. Shunt conductance and susceptibility of each distribution segment are overlooked.

For power attribute analysis, the bus voltage magnitude deviation is the most important indicator. Significant disruptions in the voltage profile indicate a poor image of the system. Equation (21) is used to determine the 24-hour average voltage deviation for each bus.

$$V_{\text{deviation}} = \sum_{t=1}^{24} \sum_{i=1}^{\text{NB}} \frac{|V_{\text{rated}} - V_i|}{V_{\text{rated}}} \quad (21)$$

2.2. Disseminated Sources of Energy

DERs must be considered in the design of the distribution system, both in terms of generation and operation. These people are the network's director generals (DG). EVs are sometimes referred to as "gridable" vehicles because they may help the grid with its electrical needs[32][33]. Electric vehicle (EV) batteries are charged and discharged up to the designated maximum and minimum ranges when the network is not in use. By incorporating electric vehicles, thermal plant emissions can be reduced and system dependability increased [34][35].

There have been considerations for both renewable and nonrenewable DERs to communicate information with the distribution control centre in this study (DCC) [36]. If the aggregators' data is correct, DCC will transport electrical power as seen in Figure 2. The WTGS and PVGS aggregators collect data on the system's electricity generation. Owners of gridable cars must first register their vehicles with the EV aggregator to use them. They can then make use of the charging and discharging options [37]. Vehicle owners are notified by the car aggregator to charge or discharge their vehicle depending on the grid's current loading circumstances [38][39]; then, the owner of an electric vehicle can reply as he deems fit. This act is thought to be a smart distribution system that might permit reliable operation and proper exploitation of DERs for the benefit of all parties involved [40]. This section also details the mathematical model for various DERs.

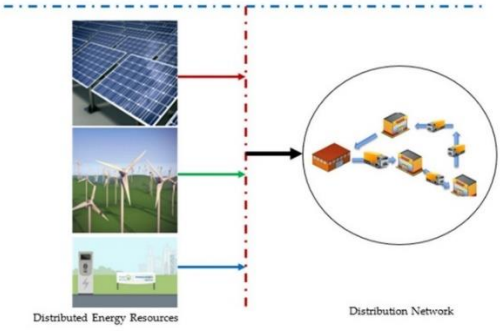

Figure 2. The suggested layout of the distribution management system

A PV module's output power is mostly determined by the concentration of solar radiation that hits it. A binomial distribution is typical for studying the behaviour of solar radiation at a certain moment in time [41]. This paradigm is related to the two straight unimodal relations; the beta probability density function (PDF), which is defined as follows, is used in both unimodal models:

$$f_b(s) = \begin{cases} \frac{\Gamma(\alpha+\beta)}{\Gamma(\alpha)+\Gamma(\beta)} \times s^{(\alpha-1)}(1-s)^{(\beta-1)} & \text{for} \quad 0 \le s \le 1, \\ & \alpha \ge 0, \beta \ge 0 \\ 0 & \text{otherwise} \end{cases} \quad (22)$$

The letter s stands for solar radiation (in kW/m^2). The two parameters of the beta distribution function fb(s), denoted by the letters α and β, respectively, can be determined using equations (23) and (24).

$$\beta = (1-\mu_s) \times \left(\frac{\mu_s \times (1+\mu_s)}{\sigma_s^2} - 1\right) \quad (23)$$

$$\alpha = \frac{\mu_s \times \beta}{1-\mu_s} \quad (24)$$

In order to calculate probabilities, the day is divided into 24 equal-sized hours, with each hour having a variable probability depending on the amount of solar radiation present at that precise instant. To determine how long each hour will last, the historical data is revisited to determine the number of days. Theoretically, there are 20 states of s, each hour with a step size of 0.05 kW/m^2. To calculate the probabilities for each of the day's 20 states using the time values of s (and s is represented in Equation (22), the PVGS output power (PV_{out}) for that given hour is calculated as a result using equation (25).

$$\mathrm{PV_{out}}(s) = N \times F_F \times V_y \times I_y \quad (25)$$

$$V_y = V_{oc} - V_k \times T_{cy} \quad (26)$$

$$I_y = s\left[I_{sc} + I_k\left(T_{cy} - 25\right)\right] \quad (27)$$

$$F_F = \frac{V_{MPT} \times I_{MPT}}{V_{oc} \times I_{sc}} \quad (28)$$

$$T_{cy} = T_A + s\left(\frac{N_{OT} - 20}{0.8}\right) \quad (29)$$

where V_y and I_y illustrate the voltage and current of each panel.

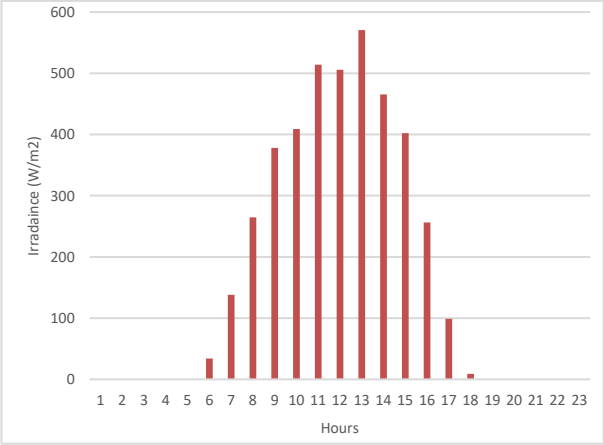

Figure 3. Irradiance data

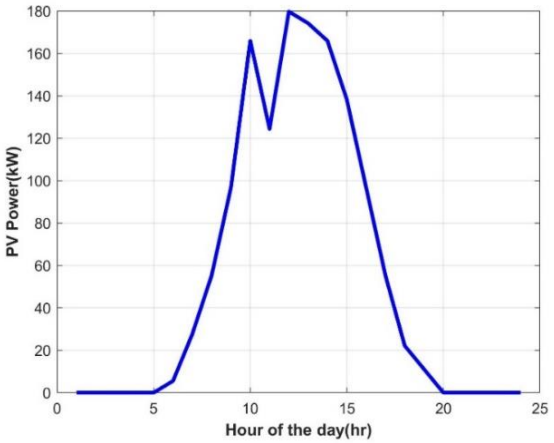

Figure 4. Power Production of Solar PV

PVGS's total anticipated output power (EOP) may be calculated at any point in time t using the formula (30).

$$\mathrm{EOP_{PV}}(t) = \int_0^1 \mathrm{PV_{out}}(s) \times f_b(s) ds \quad (30)$$

The Irradiance data is shown in Figure 3 while the corresponding PVGS's hourly production power is seen in Figure 4.

For each predicted period, the Rayleigh probability distribution function is used to characterize the randomness of wind velocity. This method is used in the popular Weibull probability distribution function [42].

$$f_w(v) = \left(\frac{2v}{c^2}\right) \exp\left[-\left(\frac{v}{c}\right)^2\right] \quad (31)$$

The scaling factor c can be calculated using Equation (32) as an average wind speed (vm) that mathematically expressed in Equation (33).

$$v_m = \int_0^\alpha v f_w dv = \int_0^\alpha \left(\frac{2v^2}{c^2}\right) \exp\left[-\left(\frac{v}{c}\right)^2\right] dv = \frac{\sqrt{\pi}}{2} c \quad (32)$$

$$c = 1.128 v_m \quad (33)$$

A 24-hour time period is used to construct the PDF, with the probability assigned to each hour based on the wind speed. On the basis of past data, we can calculate the day's hourly μw and σw. There are 24 levels of wind speed every hour, each increasing by 1 m/s. With 24 states, the probability values are calculated for each hour of the day from the w values as mentioned in Equation (31). Accordingly, the wind turbine's output power for that hour is calculated using Equation (34).

$$P_w(v) = \begin{cases} 0, & 0 \le v_{aw} \le v_{cin} \\ P_{rated} \times \frac{v_{aw} - v_{cin}}{v_{rt} - v_{cin}}, & v_{cin} \le v_{aw} \le v_{rt} \\ P_{rated}, & v_{rt} \le v_{aw} \le v_{cof} \\ 0, & v_{cof} \le v_{aw} \end{cases} \quad (34)$$

At each given time (t), the $\mathrm{EOP_{WT}}$ may be calculated using Equation (35).

$$\mathrm{EOP_{WT}}(t) = \int_0^1 P_w(v) \times f_w(v) dv \quad (35)$$

The EOP of a wind turbine may be calculated using Equations (31)- (35). Each hour is shown in Figure 5 by the wind speed for 24 hours, and Figure 6 depicts the WTGS's hourly produced output power.

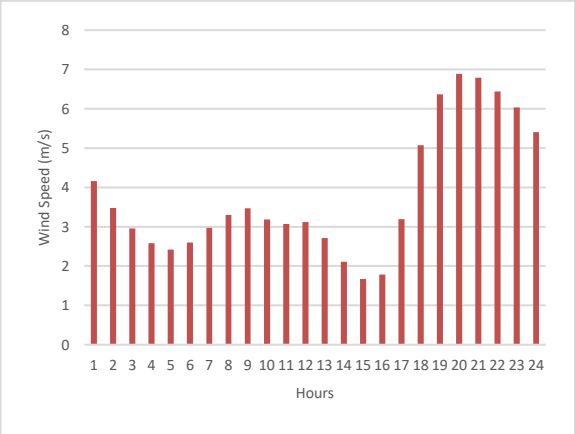

Figure 5. Wind speed at 50 meters

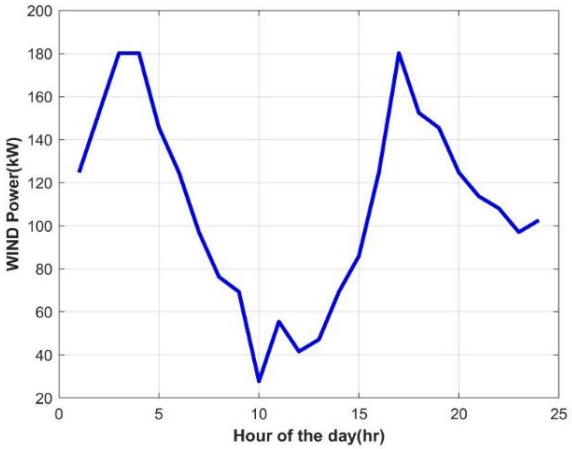

Figure 6. Power Production of Wind Turbine Generator

In this study, grid-capable vehicles are viewed as load during off-peak times when a system needs to charge EV batteries, but during peak times, they provide power back to the grid to satisfy load requirements (seemingly behaving like a DG). The deregulation of the power supply now controls the price of electricity on the market. EV owners can set up the charging and discharging of their vehicles in a way that maximizes earnings. In conclusion, the hourly charging and discharging power of EVs is calculated using formulas in Equations (36) and (37), respectively.

$$P_{\mathrm{dch}}(t) = \mu_{\mathrm{vcap}}\left[\varphi_{\mathrm{pre}} - \varphi_{min}\right] N_{\mathrm{Ev}(dch)}(t) \quad (36)$$

$$P_{\mathrm{ch}}(t) = \mu_{\mathrm{vcap}}\left[\varphi_{\mathrm{dep}} - \varphi_{\mathrm{pre}}\right] N_{\mathrm{Ev(ch)}}(t) \quad (37)$$

For charging and discharging ratings, a minimum and maximum range (φmin/φmax) should be kept. The battery life of electric vehicles (EVs) can be increased using this technique.

2.3. Minimization of Power Loss, Costs, and Emissions Generation

The implementation of an optimization algorithm is necessary to discover a suitable solution to the problem of distribution system planning. If all of the restrictions are met, then, this optimum solution may be found by picking the relevant decision variables. It is essential to use DERs to reduce power loss, overall cost, and pollution creation to a substantial degree (DERs are crucial). No power source may be used unless the exact position and size are known. ANNs and COA are used because of their power and capacity to predict the best possible results. The appropriate placements and power ratings of various power sources are determined under unpredictable load and power source conditions. So, in this distribution system planning problem, the locations and sizes are selected as choice factors. In this regard, it is clear that this method is acceptable and effective for addressing this common nonlinear optimization problem and achieving superior results.

2.3.1. Overview of Chameleon Optimization Algorithm & Artificial Neural Network

Braik suggested COA in 2021, making it one of the most recent metaheuristics. Using this technique, you may simulate the chameleon's hunting and food-finding process. As chameleons can change colour to blend in with their surroundings, they are a highly specialized species. Because they can adapt to a variety of environments, chameleons can exist in a variety of habitats including lowlands, mountains, deserts, and semi-deserts. Tracking prey, following prey, and striking prey are all phases in their food-hunting process. Step-by-step instructions for this method may be found in the ensuing sub-sections [43].

To begin the optimization process, COA produces an initial population that is generated at random. Chameleons of the species' size n are created in an optimization problem, where each member of the population represents an alternative. Using Equation (38), the chameleon's location in the search area (y_t^i) is determined.

$$y_t^i = \left[y_{t,1}^i, y_{t,2}^i, \ldots . y_{t,d}^i\right] \quad (38)$$

The d indicates the location of the chameleon in i= 1,2... t iterations.

The number of chameleons in the search space and the problem dimension is used to produce the starting population.

$$y^i = l_j + r\left(u_j - l_j\right) \quad (39)$$

A random number, ranging from 0 to 1, is used to randomize the initial vector of the ith chameleon's search space, uj, and lj, correspondingly. The quality of the solution is evaluated at each new position using the objective function.

It is possible to classify chameleon movement patterns while searching based on the approach of position update, as shown in Equation (40).

$$y_{t+1}^{i,j} = \begin{cases} y_t^{i,j} + P_1\left(P_t^{i,j} - G_t^j\right) r_2 + P_2\left(G_t^j - y_t^{i,j}\right) r_1 \\ y_t^{i,j} + \mu(u^j - li) r_3 + l_b^j \mathrm{sign}\left(\mathrm{rand} - 0.5\right) r_1 < P_p \end{cases} r_1 \geq P_p \quad (40)$$

In this example, the t[th] iteration is represented by the value t. The i[th] chameleon in the j[th] dimension is represented by i and j. The chameleon's present and new locations are denoted by yijt and yijt+1, correspondingly.

The chameleon's best and global best locations are denoted by the prefixes $P_t^{i,j}$ and G_t^j.

A person's exploratory prowess is determined by two positive integers called P_1 and P_2. Randomly generated integers r_1, r_2, and r_3 range from 0 to 1. It's possible to generate any random integer between 0 and 1 by using the index i. The likelihood of a chameleon detecting prey is given by the parameter P_p. sign (rand -0.5) can be either 0 or 1, depending on the influence it has on the direction of exploitation and exploration. Chameleons can rotate their eyes to see where their prey is hiding. They are able to see the prey in all directions thanks to this spinning characteristic. The following are the steps that follow:

The location of the prey is determined by a rotation matrix, and the situation of the chameleon is updated using the rotation matrix at the center of gravity. Then, they are returned to where they were when they first appeared.

When their victim gets too close, chameleons attack. Chameleons that are closest to their prey are considered to be the greatest. This chameleon uses its tongue to attack the prey. Chameleons benefit from their ability to double the length of their tongue. Because of this ability, the chameleon may take full advantage of the hunting space and capture prey. Equation (41) is used to determine the chameleon's speed.

$$v_{t+1}^{i,j} = wv_t^{i,j} + c_1\left(G_t^j - y_t^{i,j}\right) + c_2\left(P_t^{i,j} - y_t^{i,j}\right)r_2 \quad (41)$$

which shows the ith chameleon's new velocity in iteration t+1's jth dimension, and which shows the ith chameleon's current velocity in that dimension, as $v_{t+1}^{i,j}$.

2.3.2. Use of Artificial Neural Network

The ANN in this study is made up of one input layer, one hidden layer, and one output layer. Each layer is given a specific amount of weight [44]. Figure 7 depicts the ANN (configuration diagram).

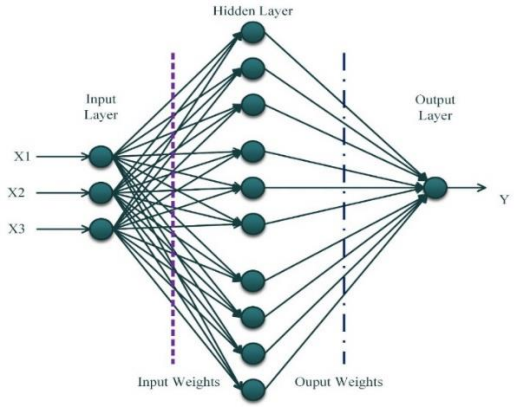

Figure 7. Structure of ANN

The output layer receives the signal from the hidden layer and sends it there. Each layer's output value is now determined by its weighted connections. Adjusting the weight value is necessary to produce the best output possible from the input signal (this is the training phase). The ANN's weights are trained via backpropagation in the suggested method. The size of the PV panel, wind turbine, and battery are among the input data for the ANN. The ANN sends out the best possible solution from the COA test results to reduce cost, emissions, and power loss.

ANN and COA are used in this study to determine the optimal parameters of the objective function and EV installation tasks simultaneously to lower power loss and overall costs; this includes the price of active electricity purchased, the price of installing and maintaining WTGS, the price of installing and maintaining PVGS, and the price of charging and discharging electric vehicles (EVs). The summary of this study is shown in Figure 8.

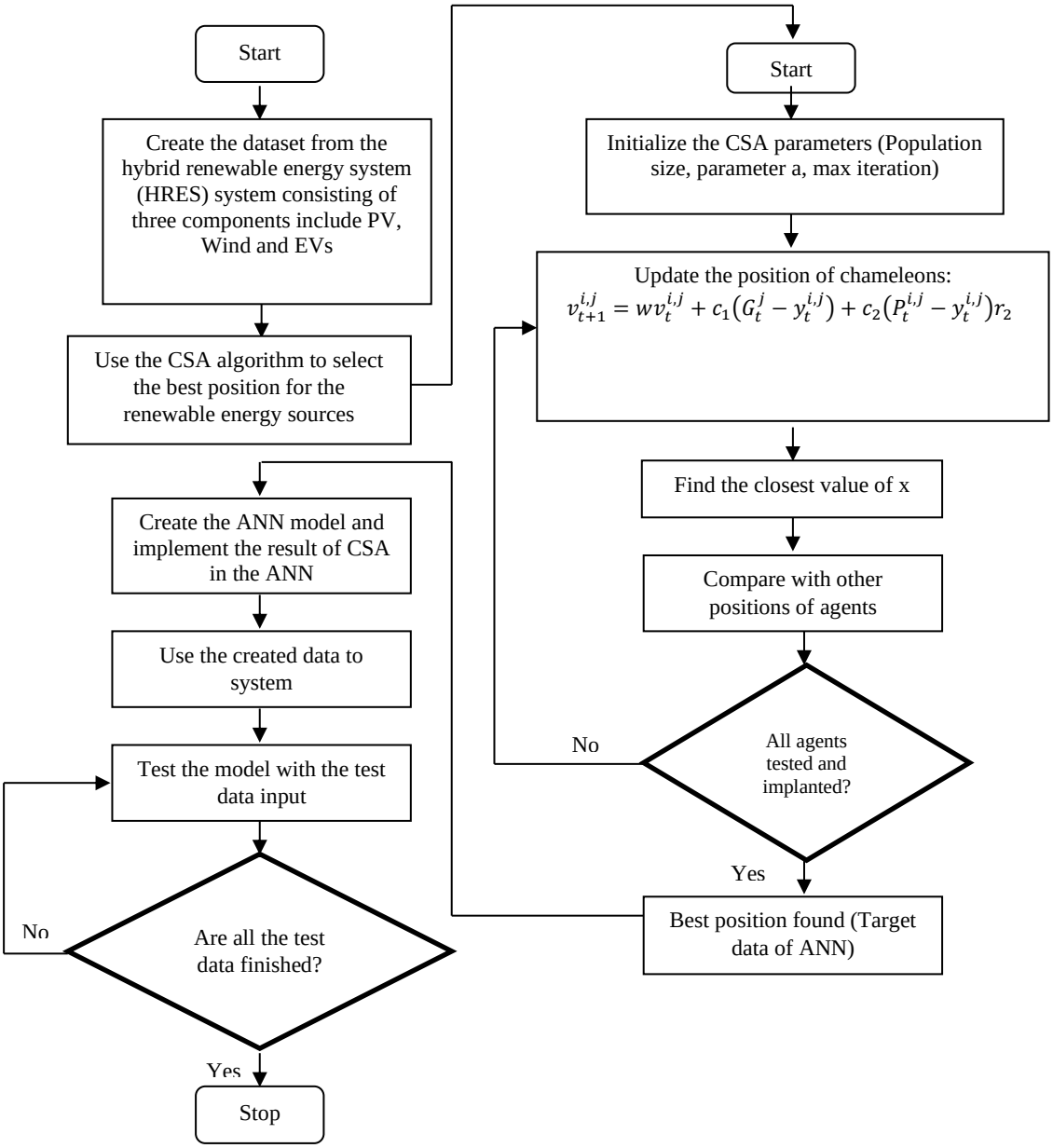

Figure 8. Flowchart of the proposed work.

3. RESULTS AND DISCUSSION

Naturally, the effects of PVGS, WTGS, and EVs on a 28-bus realistic rural distribution feeder have been evaluated in this section. At various load buses, these networks serve three distinct client types: residential, business, and industrial. The integrated method has been used to reduce the overall power loss, cost, and emissions on test systems. The spot energy market price is announced one day in advance in the deregulated electricity market. MATLAB R2022a is used for all of the simulation work, which is available on an Intel Core(i7) CPU 1.80GHz. It is mandated by IEEE 1547 standard that RESs must run at a fixed power factor that is closer in value than unity to the electrical power network. It has been agreed that renewable sources of energy can run at a maximum of 0.95 percent capacity.

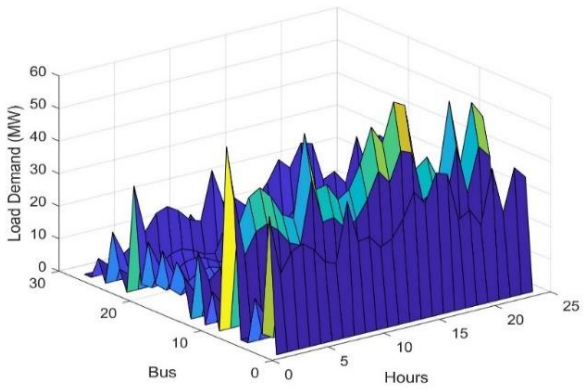

Figure 9. Uncertainty Load Power demand for 24 Hours

This 11 kV, 100 MVA system has 28 buses, 27 branches, and a main feeder with five laterals. Figure 9 depicts the

24-hour load demand uncertainty for each bus. The convergence graph for the ANN and COA is shown in Figure 10.

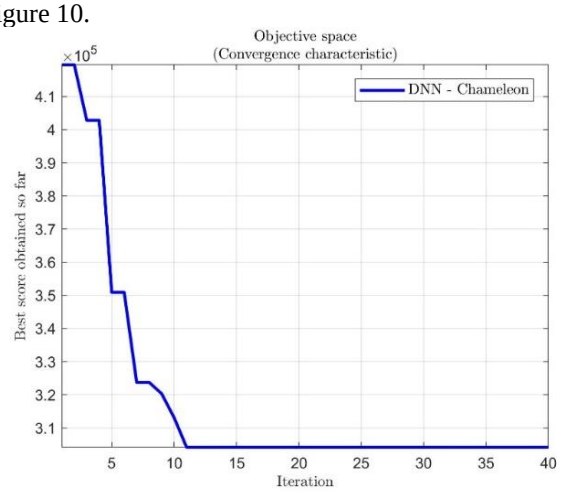

Figure 10. Convergence Graph of ANN and COA

The ANN and COA reach the global optimum value at the 11th iteration and the obtained global optimum value is 304150.16. The PV panel size is 800 with a single panel rating of 250 W and the number of wind size is 4 with a single wind generator rating of 50kW; the battery size is 12000 with a rating of 200 Ah, 12V.

This technique has been used to determine the optimal allocations, as well as the ideal number of DERs under conditions of load and EV uncertainty.

Figure 11 shows the power of the PV, wind, EV, and grid for 24 hours using ANN and COA.

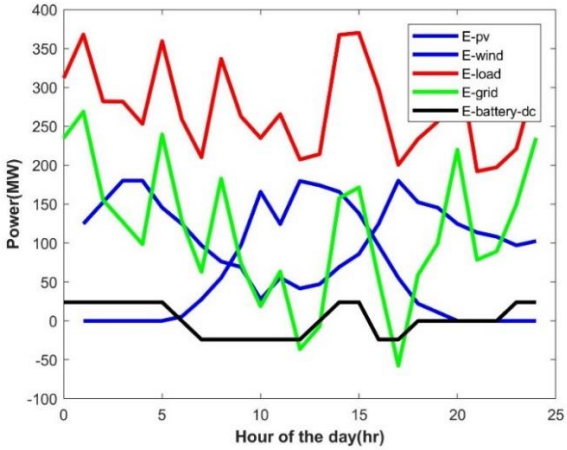

Figure 11. Power of PV, Wind, EV, and grid for 24 hours with ANN and COA

By using ANN and COA, the energy was effectively balanced based on load demand (EV demand). The variation of the state of charge of the EV is shown in Figure 12.

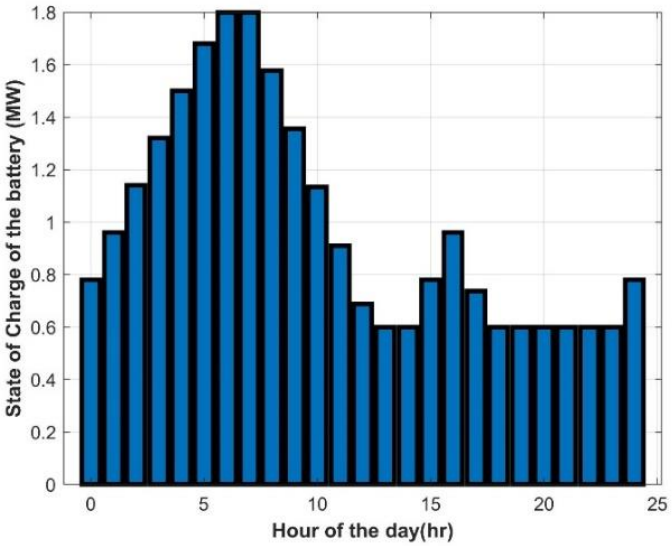

Figure 12. State of charge of the EV for 24 hours

Figure 13 shows the vehicle-to-grid and grid-to-vehicle details of the EV battery.

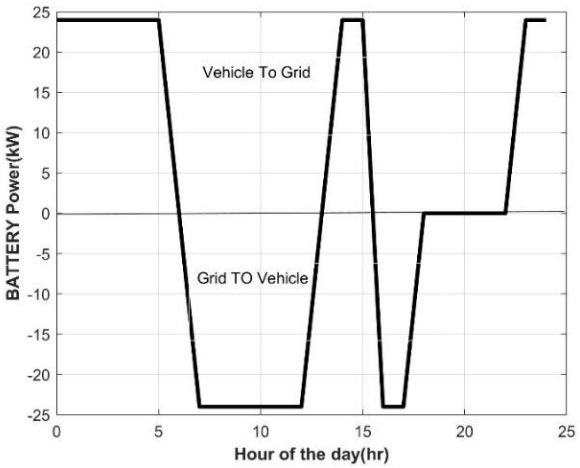

Figure 13. Grid-to-vehicle and vehicle-to-grid details of the EV battery

The EV battery supplies power to the grid from 0 to 6 hours, 13 to 16 hours, and 22 to 24 hours. However, the EV battery is charged from the grid for 6 to 12 hours and 17 to 18 hours. From 19 to 21 hours, the EV battery was idol.

The IEEE 1547 states that for renewable energy sources to operate efficiently with respect to the power grid, their fixed power factor must be closer to unity. Numerous electrical power companies and independent power providers claim that renewable energy sources can already operate at a maximum mode of 0.95. The power factor is altered to examine the effects of renewable energy sources; for this case, many cases have been taken into consideration. The cost requirements for WTGS and PVGS were obtained from [25] for this work. Technical information about WTGS, PVGS, and EVs was retrieved from [45][46][47], respectively. The following case-by-case analyses of the simulation findings are discussed:

Case 1: Without any DERs integration (base case)
Case 2: Optimal WTGS, PVGS, and EV integration into the distribution system; WTGS and PVGS operate with a 0.95 leading power factor.
Case 3: Optimal WTGS, PVGS, and EV integration into the distribution system. WTGS and PVGS operate at a unity power factor.
Case 4: Optimal WTGS, PVGS, and EV integration into the distribution system. WTGS and PVGS
Operates at a 0.95 lagging power factor.
Case 1: No DER is linked to the network in this instance. This is the network's true base case. The overall real and reactive power losses of the network are 371.87 kVAr and 554.55 kW, respectively. The cost to purchase grid-supplied active power is US $3012.32. In a 24-hour period, the grid generated 92,254.18 lb/MWh of emissions.
Case 2: For ongoing instance, the ideal number of WT units are installed at the ideal bus position and the bus number is 5. Reactive and real power losses increased to 279.45 kVar and 419.70 kW respectively after the introduction of these WT units. Active power purchase from the grid costs US$1772.06, WT installation costs US$29.310.937.50, and O&M costs US$415.029.36, respectively. The total emission of a full 24 hours operation is 10.786.20 lb/MWh.
Case 3: The WT and PV arrays can be concurrently inserted into the distribution grid at ideal locations. This bus's ideal bus position is 5, while the ideal WT unit count is 36. Similar to this, bus numbers 14 and 7 are connected at the ideal location and quantity of PV modules correspondingly choose to each bus. Following inclusion, the total real and reactive power losses are 348.57 kW and 228.85 kVar, respectively. The price of active power acquired through the network was significantly reduced to USD1196.23, which is a fantastic quantity. The costs for installing and maintaining the WT are USD58.621.875.00 and USD356.058.72, respectively. In this instance, the distribution network has optimally positioned all DERs. Bus numbers 28 and 16 are the best locations for WT and PV respectively, and their respective installation and O&M costs are USD4.555.960.00 and USD316.451.87, respectively. There is a significant reduction in the influence of the 24-hour emission production.

Case 4: In this instance, the distribution network has optimally positioned all DERs. The buses with the best placements for WT and PV are 28 and 14, respectively, with the corresponding units linked to the mentioned buses being 26 and 8, respectively. Bus number 24 receives EVs arriving for charging and discharging throughout the day. EVs can charge or discharge at a given moment, but not both at once. The notion of vehicles is created at random once each hour, with a maximum of one hundred. Once DERs are taken into account, real and reactive power losses are 225.81 kW and 148.90 kVar, respectively. The cost of purchasing active power from the network is USD 2727.88. The installation, operation, and maintenance costs for the WT are USD 57.720.000.00 and USD778.273.20, respectively. In a similar vein, the price of installing a PV system and maintaining it is USD 4.891.520.00 and USD 442.821.78, respectively. When compared to alternative combinations, the addition of WT, PV, and EVs significantly reduced the system's overall cost (cases). The amount of emissions created over a 24-hour period is higher than in Case 3 since the system took more active power from the grid to charge the EVs. The net financial gain for the car owner with EVs is USD 162.22.

The detailed numerical results for each scenario, including their unique comparison, are shown in Table 1. The table presents the impact of adding DERs on real power loss, reactive power loss, pollution created, and the cost of active electricity purchased from the network over a 24-hour period.

Table 1. Numerical results for each scenario, including their unique comparison

Cases	∑ Ploss (kW)	% Ploss Reduction	∑ Qloss (kVAr)	∑ Purchased real Power cost ($)	WT installation cost ($)	WT O&M cost ($)	PV installation cost ($)	PV O&M cost ($)	∑Emission (lb/kWh)
Case 1 (CSA)	554.55	-	371.87	3706.20	-	-	-	-	20.952.00
Case 1 (ACO)	525.26	-	343.25	3402.34	-	-	-	-	18.478.00
Case 2 (CSA)	419.70	24.32	279.45	1772.06	29.310.937.50	415.029.36	7.361.640.00	172.018.07	10.786.20
Case 2 (ACO)	398.23	23.44	246.76	1657.22	30.429.660.00	435.120.26	7.998.840.00	182.148.00	9.666.00
Case 3 (CSA)	348.57	37.14	228.85	1196.23	58.621.875.00	356.058.72	4.555.960.00	316.451.87	7.030.67
Case 3 (ACO)	375.34	38.24	244.25	1226.45	59.421.673.00	378.150.00	4.789.230.00	333.852.24	6.120.67
Case 4 (CSA)	225.81	59.28	148.90	2727.88	57.720.000.00	778.273.20	4.891.520.00	442.821.78	4.884.50
Case 4 (ACO)	246.23	57.24	132.23	3677.33	58.340.050.00	784.262.20	4.991.950.00	463.995.00	4.286.00

The results were compared with the ant colony optimization (ACO) [5] method and the results showed that CSA performed better than the ACO method.

For Case 1, the maximum real power loss was around 554.55 kW, the maximum reactive power loss was around 371.87 kVAR, and the maximum purchased active cost was around $ 3706.20. The voltage deviation maximum was around 0.07 pu. From the simulation, the proposed ANN and COA are well suited for optimizing the power loss, generation cost, and emission cost in the 28-bus system.

Stakeholders in the energy industry can benefit from the use of a Practical Radial Distribution Feeder for Techno-Economic in Distributed Energy Resources (DERs) based on ANN and the COA in the following ways:

- Improved power loss reduction: The table details the total power loss (Ploss) and the percentage reduction in power loss (% Ploss Reduction) for different cases. By using the Practical Radial Distribution Feeder with ANN and the COA, stakeholders can achieve significant reductions in power loss, leading to improved system efficiency and cost savings.
- Enhanced cost-effectiveness: The table also includes the total cost of purchased real power for each case. By optimizing the DERs using the proposed approach, stakeholders can reduce their reliance on purchased real power, resulting in cost savings. The algorithm takes into account techno-economic factors to optimize the system and minimize expenses associated with power purchases.
- Reduced environmental impact: The table presents the total emissions (lb/kWh) for each case. By utilizing the Practical Radial Distribution Feeder with ANN and the COA, stakeholders can achieve lower emissions through better utilization of DERs. This contributes to environmental sustainability and aligns with the industry's efforts to reduce carbon footprint and promote clean energy.
- Efficient utilization of DERs: The optimization approach leverages ANN and the COA to maximize the utilization of DERs, such as wind turbines (WT) and photovoltaic (PV) systems [48]. The algorithm determines the optimal installation and operation of these resources, considering factors like installation cost, operation and maintenance (O&M) cost, and overall system performance. This enables stakeholders to extract the maximum benefits from their DER investments.
- Techno-economic analysis: The use of ANN and the COA allows for comprehensive techno-economic analysis, as reflected in the table. Stakeholders can make informed decisions based on cost parameters such as installation cost, O&M cost, and overall system performance. This analysis facilitates better planning, optimization, and resource allocation, ultimately leading to improved profitability and project success.

In summary, the utilization of a Practical Radial Distribution Feeder for Techno-Economic in DERs based on ANN and the COA offers stakeholders in the energy industry significant advantages, including reduced power loss, improved cost-effectiveness, lower environmental impact, efficient DER utilization, and comprehensive techno-economic analysis. These benefits contribute to a more sustainable and optimized energy system.

4. CONCLUSION

This study evaluates whether DER integration into the distribution system is technologically, economically, and ecologically feasible. In order to solve this issue with distribution system planning, the ideal placements and sizes of PVGS, WTGS, and EVs were determined for 28 bus networks using the ANN and COA. The purchase cost of EV active power, voltage variation, minimum system voltage, emission level, and energy cost were all dramatically decreased after RESs and EVs were integrated. Charging/discharging a vehicle's battery for economic benefit is a common practice among EV owners. As a result, the grid's off-peak period will see an increase in system demand. For the most common optimization problems, the ANN and COA simulation results were satisfactory. In Case 1, CSA and ACO had similar results for Ploss, Qloss, purchased real power cost, and emissions. However, in Case 2 and beyond, CSA showed better performance with a decrease in Ploss (419.70 kW), Qloss (279.45), and emissions (10.786.20lb/kWh) compared to ACO, along with reduced costs for WT installation, WT O&M, PV installation, and PV O&M. As the cases progress, CSA consistently exhibit superior outcomes in terms of Ploss reduction, Qloss reduction, emission reduction, and cost savings, making it a favorable approach for optimizing the system. The method has also been shown to be effective at finding the optimal outcome with less iterations. The behavior of PEV owners who charge and discharge their vehicles towards getting financial advantages may lead to a rise in the demand for load during off-peak network hours. Emissions, total costs, and power loss are all significantly reduced when the distribution network's combined effects of DERs are considered.

DECLARATION OF ETHICAL STANDARDS

The authors of this article declare that the materials and methods they use in their studies do not require ethics committee permission and/or legal-specific permission

AUTHORS' CONTRIBUTIONS

Jemaa BOJOD: Performed the experiments and analyse the results and Wrote the manuscript.

Bilgehan ERKAL: Performed the experiments and analyse the results.

REFERENCES

[1] E. A. Sharew, H. A. Kefale, and Y. G. Werkie, "Power Quality and Performance Analysis of Grid-Connected Solar PV System Based on Recent Grid Integration Requirements," ***Int. J. Photoenergy***, (2021).

[2] B. Xiao, H. Zhu, S. Zhang, Z. OuYang, T. Wang, and S. Sarvazizi, "Gray-Related Support Vector Machine Optimization Strategy and Its Implementation in Forecasting Photovoltaic Output Power," ***Int. J. Photoenergy***, (2022).

[3] A. Ab-BelKhair, J. Rahebi, and A. Abdulhamed Mohamed Nureddin, "A Study of Deep Neural Network Controller-Based Power Quality Improvement of Hybrid PV/Wind Systems by Using Smart Inverter," ***Int. J. Photoenergy***, (2020).

[4] M. Nemati, M. Braun, and S. Tenbohlen, "Optimization of unit commitment and economic dispatch in microgrids based on genetic algorithm and mixed integer linear programming," ***Appl. Energy***, 210, 944–963, (2018).

[5] K. S. Swarup, "Ant colony optimization for economic generator scheduling and load dispatch," in ***Proceedings of the 6th WSEAS International Conference on Evolutionary Computing, Portugal,*** 167–175,(2005).

[6] N. Karmakar and B. Bhattacharyya, "Hybrid intelligence approach for multi-load level reactive power planning using VAR compensator in power transmission network," *Prot. Control Mod. Power Syst.*, 6(1): 1–17, (2021).

[7] A. A. M. Nureddin, J. Rahebi, and A. Ab-BelKhair, "Power Management Controller for Microgrid Integration of Hybrid PV/Fuel Cell System Based on Artificial Deep Neural Network," **Int. J. Photoenergy,** (2020).

[8] M. Al-jumaili, J. Rahebi, A. Akbas, and A. Farzamnia, "Economic dispatch optimization for thermal power plants in Iraq,"2***017 IEEE 2nd International Conference on Automatic Control and Intelligent Systems (I2CACIS)***, 140–143,(2017).

[9] K. LaCommare and C. Marnay, "Microgrids and heterogeneous power quality and reliability," ***Int. J. Distrib. Energy Resour.***, 4, no. LBNL-777E, (2007).

[10] E. Serban and H. Serban, "A control strategy for a distributed power generation microgrid application with voltage-and current-controlled source converter," ***IEEE Trans. Power Electron.***, 25(12):2981–2992, (2010).

[11] R. Majumder, A. Ghosh, G. Ledwich, and F. Zare, "Power management and power flow control with back-to-back converters in a utility connected microgrid," ***IEEE Trans. Power Syst.***, 25(2):821–834, (2009).

[12] N. Amjady, F. Keynia, and H. Zareipour, "Short-term load forecast of microgrids by a new bilevel prediction strategy," ***IEEE Trans. Smart Grid,*** vol. 1(3):286–294, (2010).

[13] H. Sajir, J. Rahebi, A. Abed, and A. Farzamnia, "Reduce power losses and improve voltage level by using distributed generation in radial distributed grid," ***2017 IEEE 2nd International Conference on Automatic Control and Intelligent Systems (I2CACIS),*** 128–133,(2017).

[14] A. H. Abed, J. Rahebi, and A. Farzamnia, "Improvement for power quality by using dynamic voltage restorer in electrical distribution networks," in ***2017 IEEE 2nd International Conference on Automatic Control and Intelligent Systems (I2CACIS)***, 122–127,(2017).

[15] D. K. Khatod, V. Pant, and J. Sharma, "Evolutionary programming based optimal placement of renewable distributed generators," ***IEEE Trans. Power Syst.***, 28(2): 683–695, (2012).

[16] Y. M. Atwa and E. F. El-Saadany, "Probabilistic approach for optimal allocation of wind-based distributed generation in distribution systems," ***IET Renew. Power Gener.***, 5(1):79–88, (2011).

[17] Y. M. Atwa and E. F. El-Saadany, "Optimal allocation of ESS in distribution systems with a high penetration of wind energy," ***IEEE Trans. Power Syst.***,25(4): 1815–1822, (2010).

[18] Y. M. Atwa, E. F. El-Saadany, M. M. A. Salama, and R. Seethapathy, "Optimal renewable resources mix for distribution system energy loss minimization," ***IEEE Trans. Power Syst.***, 25(1): 360–370, (2009).

[19] N. K. Meena, S. Parashar, A. Swarnkar, N. Gupta, and K. R. Niazi, "Improved elephant herding optimization for multiobjective DER accommodation in distribution systems," ***IEEE Trans. Ind. informatics***, 14(3):1029–1039, (2017).

[20] C. Mateo, P. Frías, and K. Tapia-Ahumada, "A comprehensive techno-economic assessment of the impact of natural gas-fueled distributed generation in European electricity distribution networks," ***Energy***, 192, 116523, (2020).

[21] Z. Ullah, M. R. Elkadeem, S. Wang, S. W. Sharshir, and M. Azam, "Planning optimization and stochastic analysis of RE-DGs for techno-economic benefit maximization in distribution networks," ***Internet of Things,*** 11,100210, (2020).

[22] M. Dixit, P. Kundu, and H. R. Jariwala, "Techno-economic analysis-based optimal incorporation of distributed energy resources in distribution network under load uncertainty," ***Int. J. Ambient Energy,*** 42(6):605–611, (2021).

[23] M. Dixit, P. Kundu, and H. R. Jariwala, "Incorporation of distributed generation and shunt capacitor in radial distribution system for techno-economic benefits," ***Eng. Sci. Technol. an Int. J.***, 20(2): 482–493, (2017).

[24] K. Hesaroor and D. Das, "Annual energy loss reduction of distribution network through reconfiguration and renewable energy sources," ***Int. Trans. Electr. energy Syst.***, 29(11):e12099, (2019).

[25] A. Maleki, M. G. Khajeh, and M. Ameri, "Optimal sizing of a grid independent hybrid renewable energy system incorporating resource uncertainty, and load uncertainty," ***Int. J. Electr. Power Energy Syst.***, 83, 514–524, (2016).

[26] W. Hu, C. Su, Z. Chen, and B. Bak-Jensen, "Optimal operation of plug-in electric vehicles in power systems with high wind power penetrations," ***IEEE Trans. Sustain. Energy***, 4(3): 577–585, (2013).

[27] S. Suthar, S. H. C. Cherukuri, and N. M. Pindoriya, "Peer-to-peer energy trading in smart grid: Frameworks, implementation methodologies, and demonstration projects," ***Electr. Power Syst. Res.***, 214, 108907, (2023).

[28] R. Lazdins, A. Mutule, and D. Zalostiba, "PV Energy Communities—Challenges and Barriers from a Consumer Perspective: A Literature Review," ***Energies***, 14(16): 4873, (2021).

[29] M. A. Butturi, F. Lolli, M. A. Sellitto, E. Balugani, R.

Gamberini, and B. Rimini, "Renewable energy in eco-industrial parks and urban-industrial symbiosis: A literature review and a conceptual synthesis," ***Appl. Energy***, 255, 113825, (2019).

[30] M. A. Hannan, M. Faisal, P. J. Ker, R. A. Begum, Z. Y. Dong, and C. Zhang, "Review of optimal methods and algorithms for sizing energy storage systems to achieve decarbonization in microgrid applications," ***Renew. Sustain. Energy Rev.***, 131, 110022, (2020).

[31] S. M. Zahraee, N. Shiwakoti, and P. Stasinopoulos, "Biomass supply chain environmental and socio-economic analysis: 40-Years comprehensive review of methods, decision issues, sustainability challenges, and the way forward," ***Biomass and Bioenergy***, 142, 105777, (2020).

[32] G. Sree Lakshmi, R. Olena, G. Divya, and I. Hunko, "Electric vehicles integration with renewable energy sources and smart grids," ***Advances in Smart Grid Technology*, Springer,** 397–411(2020).

[33] N. I. Nimalsiri, E. L. Ratnam, D. B. Smith, C. P. Mediwaththe, and S. K. Halgamuge, "Coordinated charge and discharge scheduling of electric vehicles for load curve shaping," ***IEEE Trans. Intell. Transp. Syst.,*** (2021).

[34] M. Kumar, S. Vyas, and A. Datta, "A review on integration of electric vehicles into a smart power grid and vehicle-to-grid impacts," ***2019 8th International Conference on Power Systems (ICPS)***, 1–5,(2019).

[35] S. Shafiq, U. Bin Irshad, M. Al-Muhaini, S. Z. Djokic, and U. Akram, "Reliability evaluation of composite power systems: Evaluating the impact of full and plug-in hybrid electric vehicles," ***IEEE Access***, 8, 114305–114314, (2020).

[36] M. Dixit, "Impact of optimal integration of renewable energy sources and electric vehicles in practical distribution feeder with uncertain load demand," ***Int. Trans. Electr. Energy Syst.,*** 30(12):e12668, (2020).

[37] A. T. Lemeski, R. Ebrahimi, and A. Zakariazadeh, "Optimal decentralized coordinated operation of electric vehicle aggregators enabling vehicle to grid option using distributed algorithm," ***J. Energy Storage***, 54, 105213, (2022).

[38] M. A. Hannan *et al.*, "Vehicle to grid connected technologies and charging strategies: Operation, control, issues and recommendations," ***J. Clean. Prod.***, 130587, (2022).

[39] T. U. Solanke, V. K. Ramachandaramurthy, J. Y. Yong, J. Pasupuleti, P. Kasinathan, and A. Rajagopalan, "A review of strategic charging–discharging control of grid-connected electric vehicles," ***J. Energy Storage***, 28, 101193,(2020).

[40] M. I. Azim, W. Tushar, T. K. Saha, C. Yuen, and D. Smith, "Peer-to-peer kilowatt and negawatt trading: A review of challenges and recent advances in distribution networks," ***Renew. Sustain. Energy Rev.,*** 169, 112908, (2022).

[41] M. A. Rogalski and M. A. Duffy, "Local adaptation of a parasite to solar radiation impacts disease transmission potential, spore yield, and host fecundity," ***Evolution (N. Y).***, 74(8):1856–1864, (2020).

[42] M. Sumair, T. Aized, M. M. A. Bhutta, F. A. Siddiqui, L. Tehreem, and A. Chaudhry, "Method of Four Moments Mixture-A new approach for parametric estimation of Weibull Probability Distribution for wind potential estimation applications," ***Renew. Energy***, 191, 291–304, (2022).

[43] M. S. Braik, "Chameleon Swarm Algorithm: A bio-inspired optimizer for solving engineering design problems," ***Expert Syst. Appl.***, 174,114685, (2021).

[44] B. Shboul *et al.*, "A new ANN model for hourly solar radiation and wind speed prediction: A case study over the north & south of the Arabian Peninsula," ***Sustain. Energy Technol. Assessments***, 46, 101248, (2021).

[45] V. Black, "Cost and performance data for power generation technologies," ***Prep. Natl. Renew. Energy Lab.***, (2012).

[46] J.-H. Teng, S.-W. Luan, D.-J. Lee, and Y.-Q. Huang, "Optimal charging/discharging scheduling of battery storage systems for distribution systems interconnected with sizeable PV generation systems," ***IEEE Trans. Power Syst.***, 28(2): 1425–1433,(2012).

[47] A. Ellis *et al.*, "Reactive power interconnection requirements for PV and wind plants–recommendations to NERC," ***Sandia Natl. Lab. Albuquerque, New Mex.***, 87185, (2012).

[48] A. Naderipour *et al.*, "Carrier wave optimization for multi-level photovoltaic system to improvement of power quality in industrial environments based on Salp swarm algorithm," ***Environ. Technol. Innov.***, 21, 101197, (2021).